Appl. Phys. B 85, 265–272 (2006)
DOI: 10.1007/s00340-006-2331-x

Applied Physics B
Lasers and Optics

V. ZENINARI[1,✉]
B. PARVITTE[1]
L. JOLY[1]
T. LE BARBU[1,2]
N. AMAROUCHE[3]
G. DURRY[1,2]

Laboratory spectroscopic calibration of infrared tunable laser spectrometers for the in situ sensing of the Earth and Martian atmospheres

[1] Groupe de Spectrométrie Moléculaire et Atmosphérique, UMR CNRS 6089, UFR Sciences Exactes et Naturelles, Moulin de la Housse, BP 1039, 51687 Reims CEDEX 2, France
[2] IPSL, Service d'Aéronomie, UMR CNRS 7620, 91371 Verrières-le-Buisson CEDEX, France
[3] Division Technique de l'INSU, UPS 855, 1 place Aristide Briand, 92195 Meudon CEDEX, France

Received: 31 March 2006/Revised version: 15 May 2006
Published online: 28 June 2006 •

ABSTRACT This paper reports the laboratory spectroscopic calibration of near- and mid- infrared tunable laser spectrometers used to determine in situ trace gases in the middle atmosphere of the Earth or in development for the investigation of the Martian atmosphere. The use of infrared absorption spectroscopy to measure gas concentrations requires a proper knowledge of the rotation–vibration spectra of the targeted molecules as well as a proper investigation of the tunable laser spectral emission properties. This last point is of particular importance for the use of new-generation lasers like quantum-cascade lasers or room-temperature multi-quantum wells laser diodes emitting between 2 and 3 μm. Purposely, we have developed various laboratory tunable laser set-ups to obtain accurate line strengths and pressure-broadening coefficients of atmospheric molecules and to test the performances of cutting-edge laser technology for trace gas sensing. In this paper, the spectroscopic calibration work is described. Several atmospheric applications of tunable laser are reported to stress the impact on concentration retrieval of a proper spectroscopic calibration work.

PACS 07.57.T; 93.85; 07.87

1 Introduction

Distributed-feedback continuous wave laser diodes emitting in the near infrared have demonstrated their capabilities for atmospheric sounding [1, 2]. Indeed, from 1 to 2 μm a large number of molecular species of interest in atmospheric science, for example methane at 1.65 μm, water vapor at 1.39 μm, carbon dioxide at 1.60 μm, hydrogen chloride at 1.74 μm, and hydrogen fluoride at 1.27 μm, exhibit rotation–vibration absorption lines that are suitable for in situ monitoring. Nowadays laser diodes in pigtailed packages with emission wavelengths that range from 1 to 2 μm are available from various suppliers. The spectral-emission properties of laser diodes make them particularly well suited for gas monitoring by infrared absorption spectroscopy. Unlike cryogenically cooled mid-infrared lead-salt laser diodes that are usually used for atmospheric sensing [3, 4], laser diode devices can be operated at room temperature. These properties have been used for field operation form several airborne or balloon operations [1, 5]. However, even if telecommunication lasers are highly efficient sources for atmospheric monitoring, a precise knowledge of the molecular parameters for the selected single transition that is scanned over by the laser is of high importance to achieve a high accuracy in the measurements. For example a variation in the line intensity of 5% leads to a direct variation of 5% on the concentration retrieval. Other parameters such as self-broadening and air-broadening coefficients may strongly influence the concentration retrieval. We will make use of H_2O data at 1.39 μm yielded in the middle atmosphere by the SDLA (Spectromètre & Diode Lasers Accordables) balloon-borne near-infrared diode laser spectrometer [1, 6] to illustrate the impact of a proper spectroscopic calibration work on the concentration retrieval.

New laser technologies are now emerging which seem quite appropriate for in-situ laser sensing. Multi-quantum wells laser diodes emitting between 2 and 3 μm are now commercially available, for instance from Nanoplus , with a stable laser emission at room temperature. We intend to use this laser technology for TDLAS (Tunable Diode Laser Absorption Spectrometer), a highly compact TDL spectrometer devoted to the in situ monitoring of the water vapor and carbon dioxide isotopes in the lower Martian atmospheres [7]. Quantum cascade lasers (QCL) are another promising source for atmospheric applications [8]. These lasers are unipolar lasers and the emitted wavelength is entirely determined by quantum confinement. The same material can be used from the mid-infrared to the THz region without having to rely on small band gap semiconductors. This type of laser is in constant evolution and its emission in the mid-infrared region where strong fundamental rovibrational transitions take place seems highly suitable for such field measurements.

In this paper we will present laboratory techniques for the precise determination of spectroscopic parameters, line strengths, self-broadening and air-broadening coefficients as well as the determination of the laser capability for gas monitoring. The studied lines are those used in the concentration retrieval by the balloon-borne instruments or space projects. These parameters are mainly compared with those of the HITRAN database [9]. In principle, the TDL spectrometer scans one selected rovibrational transition and hence the achieved inaccuracy is depending upon a proper knowledge of the mo-

✉ Fax: +33-326913147, E-mail: virginie.zeninari@univ-reims.fr

lecular parameters, i.e. line-strength, the pressure broadening effect and its temperature-dependence on the specific transition. We have often observed during our calibration work that the HITRAN database does not provide a sufficient inaccuracy for a single selected line, particularly in the near-infrared. The major part of HITRAN values are calculated ones usually based on measurements. Thus the parameters for a particular ro-vibrational line may be quite false: for example up to a 20% difference for line strengths, and up to a 50% difference for broadening coefficients, were observed for water vapor in the near-infrared spectral range. This database is in constant evolution but the user must be careful. The best solution to precisely know the individual parameters for a single line is to re-measure them with a high-resolution tunable laser spectrometer. We will show in this paper various examples of laboratory tunable laser measurements that drastically influence the concentration retrieval in the Earths atmosphere. We will also show that new instruments that are currently being developed on tunable laser technology must take into account the necessity of carefully knowing the spectroscopic parameters. Finally we will present the possibility of using a new generation of lasers, the quantum cascade lasers, to develop a new generation of instruments.

2 Laboratory measurements of spectroscopic parameters

The experimental spectra are recorded at high resolution in the laboratory with tunable diode laser (TDL) spectrometers. The experimental set-up is shown in Fig. 1. The laser sources are identical to those mounted on the instruments. The usual average output power is ~ 1 mW, and the laser linewidth is usually less than 10 MHz. We checked that the apparatus function of the spectrometer is negligible by recording low-pressure spectra. In these conditions the lineshape could be fitted by a simple Gaussian curve having a Doppler width in good agreement with the theoretical value. Moreover there are no mode-hops over the tunability range. The continuous tuning range (at constant temperature) is usually within 3 cm^{-1}.

The laser wavelength is temperature-stabilized by means of a Peltier thermo-element and is driven by a low noise current supply. Nevertheless liquid nitrogen cooling is required for the QCL used in this study. A low-frequency triangular ramp at 100 Hz is used to scan the laser over the selected absorption lines by modulation of the driving current. The laser beam (channel A) is usually collected by a lens and is separated into two parts via a beam splitter. The reflected beam (channel B) is coupled with a spherical Fabry–Pérot (SFP) etalon used for relative frequency calibration with a free spectral range of 0.01 cm^{-1}. The SFP gives good insight into the linearity of the tuning of the laser emission frequency; the signal from the SFP further permits detection of mode jumps over the laser spectral tunability range. The second beam (channel C) is passed through a gas cell filled with high purity of the gas under study. When using pigtailed laser diodes, the fiber is junctioned to a 50/50 fused coupler. The main beam is coupled with the SFP and the remaining part of the beam passes through the absorption cell. Both beams are focused on photodetectors adapted to the laser wavelength. The data acquisition is made with a digital oscilloscope (10 ms per spectrum, 11 bit resolution). The spectra are usually averaged 10 times in order to enhance the signal to noise ratio. We use a computer to collect all the data. The whole set-up may take place in a closed box, filled with dry nitrogen at atmospheric pressure in order to minimize the absorption by ambient water vapor when necessary.

Various cells have been laboratory-designed to fulfill all requirements in order to adapt the cell length to the gas absorption. The laboratory is equipped with single pass cells 10 cm or 20 cm long, a White type multipass cell that provides from 1 m to 10 m path lengths and another White type multipass cell designed to obtain a 48 m length cell. The first White type cell can be used for measurements between room temperature and $-60°C$. The second White type cell permits obtaining of a path length which can be adjusted between 10 and 70 m. The gas samples are usually supplied by Air Liquide with a stated purity of more than 99.99%.The gas pressure is measured with an uncertainty of 0.5% using an MKS baratron manometer with a full scale of 10 Torr or 1000 Torr. Several spectra at various pressures are usually recorded. An example of a high resolution recorded spectra of H_2O in the 1.39 μm region is presented in Fig. 2 with the etalon fringes.

To retrieve the absolute intensity of the line we apply a nonlinear least-squares fit to the molecular transmission

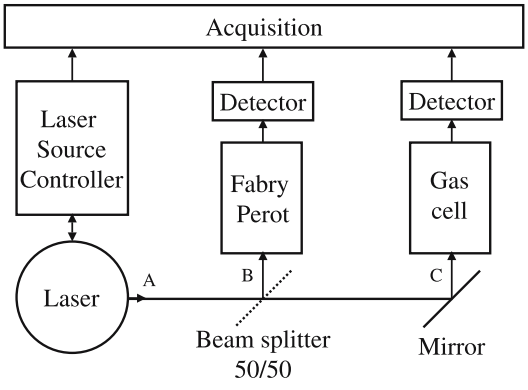

FIGURE 1 Schematic laboratory experimental set-up

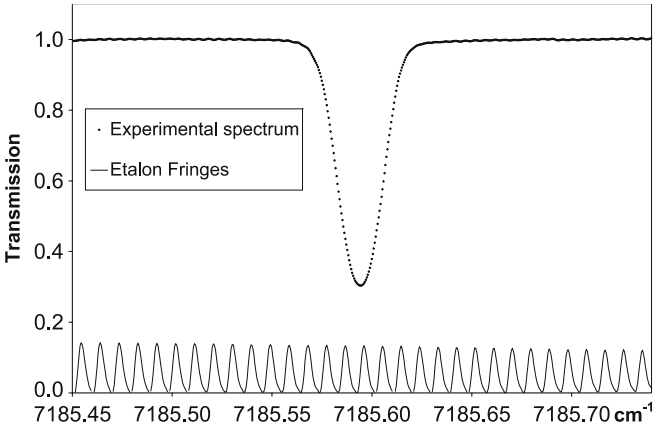

FIGURE 2 Example of recorded transmission spectrum for the $6_{60} \leftarrow 6_{61}$ transition of the $\nu_1 + \nu_3$ band of H_2O at 7185.596 cm^{-1}. Pressure is 1.5 mbar, temperature is 293K and absorption path length is 10 m. The Fabry–Pérot interferometer fringes are shown at the *bottom*

using a Voigt-profile for the modeling of the line shape. The molecular transmission $T(\sigma)$ is obtained from the two signals in two steps. First, the Fabry–Pérot signal is used to perform the frequency scaling with a polynomial interpolation on the interference fringes. In a second step, we retrieve the molecular transmission from the direct spectrum A using the relation:

$$A = A_0 T(\sigma)\,. \tag{1}$$

A_0 is what would be the laser flux in the absence of absorber in the cell. A_0 is obtained from A with a polynomial interpolation over the full transmission region. The line intensity $S(T)$ is related to the molecular transmission through the Beer–Lambert law:

$$T(\sigma) = I_{\mathrm{T}}(\sigma)/I_0(\sigma) = \exp\left[-k(\sigma, T, p)nl\right]\,, \tag{2}$$

where n is the density of absorbing molecules on the optical path of length l, and the absorption coefficient $k(\sigma, T, p)$ at temperature T and for a gas pressure p is modeled using the Voigt profile:

$$k(\sigma, T, p) = S(T)B\frac{y}{\pi}\int\limits_{-\infty}^{+\infty}\frac{\exp\left(-t^2\right)}{y^2+(x-t)^2}\mathrm{d}t\,, \tag{3}$$

with $B = \frac{\sqrt{\ln 2}}{\gamma_{\mathrm{Dop}}\sqrt{\pi}}$, $y = \sqrt{\ln 2}\frac{\gamma_{\mathrm{Col}}}{\gamma_{\mathrm{Dop}}}$, $x = \sqrt{\ln 2}\frac{\sigma-\sigma_0}{\gamma_{\mathrm{Dop}}}$ where $S(T)$ is the line intensity at temperature T, σ_0 is the line center wavenumber at pressure p, γ_{Dop} is the Doppler halfwidth, and γ_{Col} is the collisional halfwidth $\gamma_{\mathrm{Col}} = \gamma_{\mathrm{Self}} \times p \times c + \gamma_{\mathrm{Gas}} \times p \times (1-c)$ where γ_{Self} is the self-broadening coefficient and c the concentration when air-broadening coefficients are measured.

The Voigt profile cannot be expressed in analytical form but may be expressed as the real part of the complex probability function $W(x, y)$ defined by:

$$W(x, y) = \frac{\mathrm{i}}{\pi}\int\limits_{-\infty}^{+\infty}\frac{\exp\left(-t^2\right)}{x+\mathrm{i}y-t}\mathrm{d}t\,, \tag{4}$$

which can be evaluated using the Humlicek algorithm [10].

The line intensity at temperature T is related to the intensity S_0 at the reference temperature $T_0 = 296$ K by:

$$S(T) = S_0\frac{Q_{\mathrm{v}}(T_0)}{Q_{\mathrm{v}}(T)}\frac{Q_{\mathrm{r}}(T_0)}{Q_{\mathrm{r}}(T)}\exp\left\{-\frac{hcE_0}{k}\left(\frac{1}{T}-\frac{1}{T_0}\right)\right\}\,, \tag{5}$$

where E_0 is the lower level energy expressed in cm^{-1}, Q_{v} and Q_{r} are respectively the vibrational and rotational partition functions and are calculated using the expressions given by Gamache et al. [11]. The line intensities are measured in units of $\mathrm{cm}^{-1}/(\mathrm{molecule/cm}^2)$ at the temperature of each spectrum, using the total measured pressure without correction for isotopic abundance. This line intensity for each spectrum is then standardized to $T = 296$ K using (5) so that the measurements from the spectra of each transition could be averaged. The corresponding intensities are compared with the HITRAN database values [9]. Line intensity appropriate for a gas of the pure isotopomer can be obtained by dividing the HITRAN value by the isotopic fraction. Our uncertainty is usually approximately 2%. This error corresponds to one standard deviation obtained by averaging the measurements at 296 K for each line. The half-widths of the lines are issued from the fitting procedure and plotted vs. pressure. The slope of the linear straight regression line gives the broadening coefficient.

For numerous spectra, we observe that the Voigt profile is not sufficient to correctly describe the line profile. In order to obtain a better residual we usually fit our measurements with other line profile models. The model developed by Rautian and Sobel'man [12] that take into account Dicke narrowing leads to the expression:

$$k_{\mathrm{R}}(\sigma, T, p) = S(T)B\,\mathrm{Re}\left[\frac{W(x, y+z)}{1-\sqrt{\pi}zW(x, y+z)}\right]\,, \tag{6}$$

where $z = \sqrt{\ln 2}\frac{\beta}{\gamma_{\mathrm{Dop}}}$ where β is related to the collisional narrowing coefficient β_0 by $\beta = \beta_0 \times p$ and B, x and y have their previous meaning. The other model developed by Galatry [13] leads to the expression:

$$k_{\mathrm{G}}(\sigma, T, p) = S(T)B\,\mathrm{Re}\left[\frac{1}{(1/2z)+y-ix}\times M\left(1; 1+\frac{1}{2z^2}+\frac{y-ix}{z}; \frac{1}{2z^2}\right)\right]\,, \tag{7}$$

where M(... ; ... ; ...) is a hypergeometric function and B, x, y and z have their previous meaning. These models give a better agreement between the fitted profile and the experimental profile. The observed-minus-calculated residuals are usually notably reduced with these profiles, which indicates that Dicke narrowing effects are not negligible.

An example of a high resolution recorded absorption spectrum of CO_2 in the 1.88 μm region is presented in Fig. 3 with a new generation Nanoplus Laser. The experimental profile and the fitted Voigt profile are presented. The lower panels show residuals of the observed spectrum and the calculated values described by the Voigt profile (V), the Rautian–Sobel'man model (R) and the Galatry model (G). The residual between the Voigt profile and the experimental profile shows a characteristic M form. The residual using Rautian–Sobel'man or Galatry profiles is smaller. Usually, as in Fig. 3, there is no difference between the residuals obtained with Rautian–Sobel'man and Galatry models. The influence on the retrieved intensity is usually less than one percent whatever the profile. That is why atmospheric spectra are usually retrieved with a Voigt profile.

3 Application to the in situ sensing of the Earth's atmosphere

The SDLA, a near infrared tunable diode laser spectrometer operated from stratospheric balloons, was originally dedicated to the in situ measurements of H_2O and CH_4 concentrations in the upper troposphere and the lower stratosphere [1, 6]. A second instrument μSDLA [14], a compact version of SDLA, was more recently designed in order to record H_2O, CH_4 and CO_2 concentrations with balloons of the smallest size in tropical regions. The science objective consists of studying with high resolution in situ H_2O

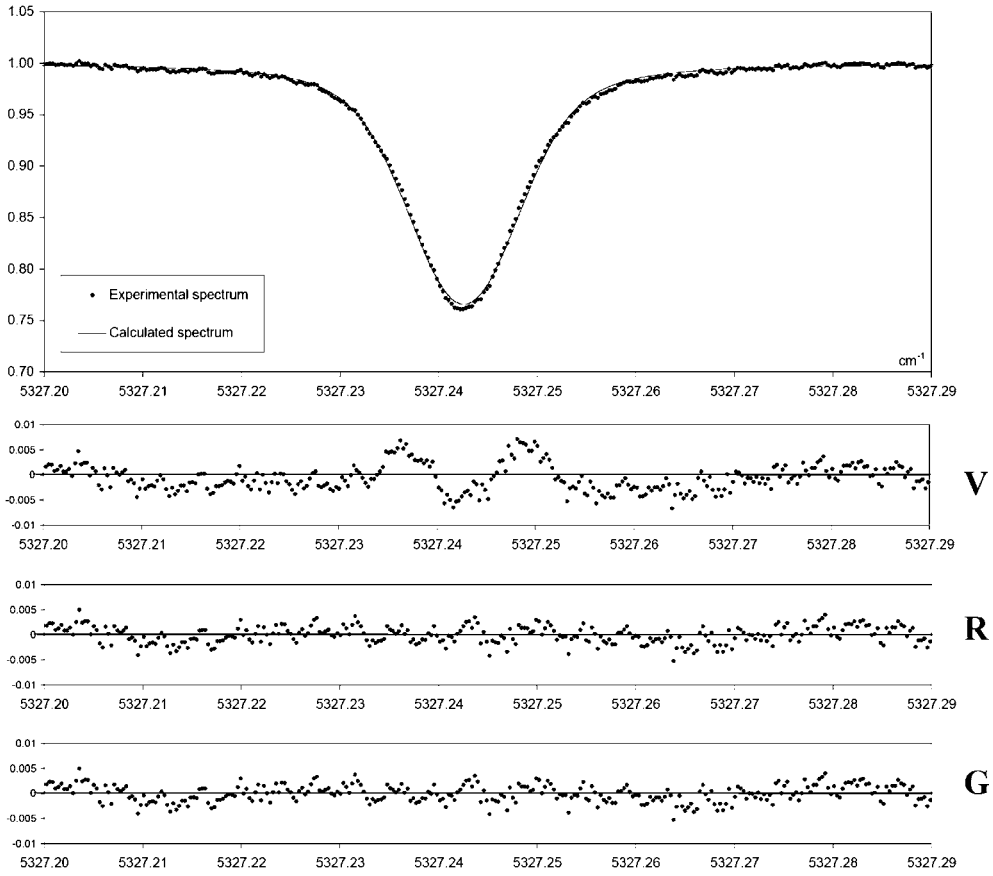

FIGURE 3 Example of recorded transmission spectrum for the R16 transition of the $(01^12)_I \leftarrow (000)$ band of CO_2 at 5327.242 cm^{-1}. The experimental profile, the fitted Voigt profile and residuals of the observed spectrum and the calculated values described by the Voigt profile (V), the Rautian model (R) and the Galatry model (G) are presented. Pressure is 23.8 mbar, temperature is 293 K and absorption path length is 69.6 m

data, the transport processes that inject and mix tropospheric H_2O in the lower tropical stratosphere which are indeed largely unknown. The μSDLA uses three telecommunication distributed-feedback InGaAs diode lasers emitting, respectively, at 1.393 μm (Thales-LCR), 1.602 μm (Anritsu) and 1.653 μm (Sensors unlimited) to record in situ atmospheric spectra of H_2O, CO_2 and CH_4. The capability of DFB laser diodes to monitor trace gas in the middle atmosphere was demonstrated during the numerous stratospheric flights made with these sensors.

In order to meet the scientific objectives, a precision in the concentration retrieval of less than 5% for a measurement time of 1 s is required. Hence, a precise knowledge (better than 2%) of the molecular parameters for particular ro-vibrational lines is of high importance. Scientists usually use the HITRAN database to find the spectroscopic parameters of a particular ro-vibrational line. However, the database may contain inaccurate values particularly in the near-infrared region because the lines belong to harmonic bands. This effect has been demonstrated in [15–17] where spectroscopic line strength and air-broadening coefficients were measured in the laboratory. With the SDLA and μSDLA sensors, in order to compensate the decreasing of water vapor concentration with altitude, the laser wavelength is swept on four water vapor lines with increasing linestrengths belonging to the $\nu_1 + \nu_3$ band of H_2O. The CO_2 line belongs to the $(30^01) \leftarrow (000)$ band. The lines used by the SDLA are presented in Table 1.

Our laboratory results are in bad agreement with the HITRAN 2000 database: up to a 40% difference for the strength of one line of H_2O and up to 20% for some air-broadening coefficients. The influence on the atmospheric concentration retrieval can be seen in Fig. 4. At around 8 km during the descent the laser line is swept from 7182.9 cm^{-1} to 7185.5 cm^{-1}. The blue profile is obtained using HITRAN 2000 parame-

Molecule	Transition (J_{KaKc}) upper ← (J_{KaKc}) lower	σ_0 (cm^{-1})	Altitude range (km)	Line strengths (10^{-22} cm^{-1}/(molecule cm^{-2}))			Air-broadening coefficients (cm^{-1}/atm)		
				Our work	HITRAN 2000	HITRAN 2004	Our work	HITRAN 2000	HITRAN 2004
H_2O	$6_{60} \leftarrow 6_{61}$	7185.59600	5–8	7.85	7.11	7.95	0.0417	0.0505	0.0421
H_2O	$2_{12} \leftarrow 3_{13}$	7182.94955	8–14	36.9	53.0	37.5	0.0980	0.0980	0.0974
H_2O	$2_{02} \leftarrow 3_{03}$	7181.15570	> 14	142	180	150.5	0.1034	0.1031	0.1008
H_2O	$3_{03} \leftarrow 3_{22}$	7175.98675	< 5	2.59	2.27	2.71	0.1032	0.0919	0.0958
CO_2	R16	6240.10492	all	0.1771	0.1839	0.1839	0.0669	0.0734	0.0734

TABLE 1 List of the lines used by the SDLA instrument

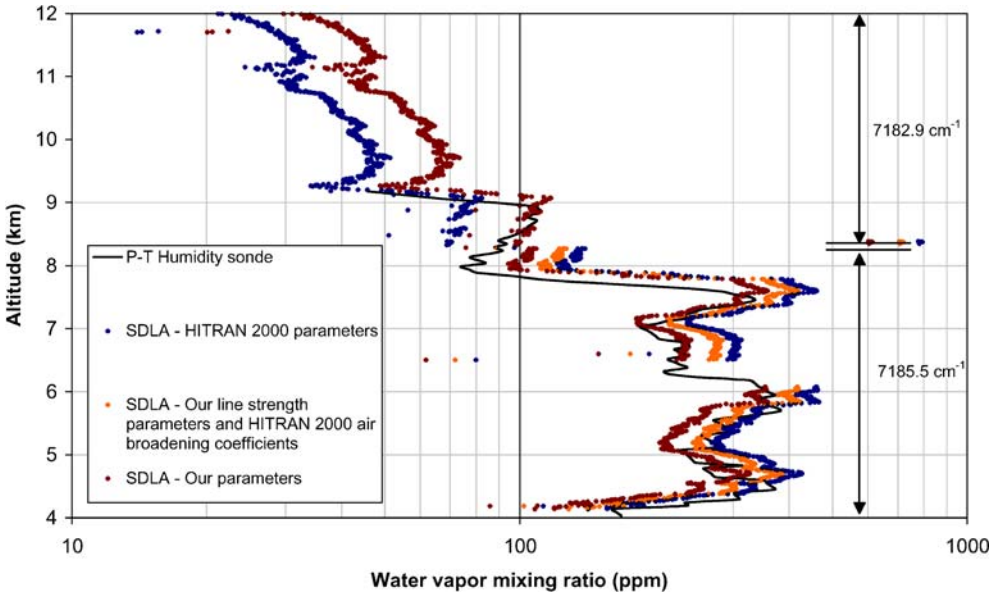

FIGURE 4 A vertical in situ concentration profile of H_2O yielded by the SDLA in southern France on 16 October 2001. The retrieval has been made with different spectroscopic parameters

ters. One can notice that the profiles do not overlap in the transition of the line sweeping. The retrieved concentration roughly changes from 70ppm up to more than 120ppm for the same altitude. This change is not so brutal using our line strength parameters and HITRAN 2000 air broadening coefficients (upper brown profile and lower orange profile). For the line at 7182.9 cm^{-1} our broadening coefficient was the same as the HITRAN one. In this case the correspondence between the SDLA retrieved profile is in good agreement with those obtained from a balloon-borne P, T-humidity meteorological sonde. The overlapping of the profiles remains not good in this case. It becomes quite perfect using our broadening coefficients (whole brown profile). It is interesting to note that the HITRAN 2004 database has been amended for H_2O lines. The maximum difference for strength and air-broadening coefficients is lower than 6% for the studied lines.

On the contrary the CO_2 parameters used for the retrieval of the CO_2 concentration with the SDLA instrument are the same in HITRAN 2000 and 2004. The difference in line strength of 4% remains between our experimental value and the database (see Table 1) value. Hence the absolute error causes by using HITRAN parameters may be 4%. This is too large to correctly reach the scientific objectives of the sensor. This experimental laser diode result has been confirmed recently by Fourier Transform measurements [18]. So the use of precisely laboratory determined parameters is of first importance for the retrieval of in situ concentrations with laser instruments.

4 Application to the in situ sensing of the Martian atmosphere

The amounts of H_2O and CO_2 in the atmosphere of Mars are much higher than in the Earths lower stratosphere. The atmosphere of Mars contains 95% carbon dioxide (360 ppmv on Earth), and its water vapor content is roughly 200 ppmv, (5 ppmv in the Earths lower stratosphere). The Martian pressure is approximately 7 hPa, and (10 hPa on Earth at 30 km). Hence, the developed laser probing technique should be also efficient for studying in-situ the lower Martian atmosphere. We have explored, with the support of the French space agency, the capability for gas sensing of a new generation of multi-quantum well GaInAsSb/GaAlAsSb laser diodes from Nanoplus emitting at room temperature in the 2–3 μm region, which cannot be reached with the standard telecommunication laser technology used with the SDLA and μSDLA instruments. This spectral region offers many opportunities: a reduced path length making it possible to construct compact spectrometers or an additional isotopic measurement of isotopologues in the lower atmosphere of Mars to address exobiology issues.

The schematic representation of the TDLAS instrument is presented in Fig. 5. The absorption path length of 1.2 m in the open atmosphere is achieved by combining a spherical mirror (focal length of 30 cm) with a flat mirror. The amount of absorbed laser energy is related to the molecular concentrations with the Beer–Lambert law. At the low Martian pressures, the collisional pressure broadening effect is almost negligible. The molecular profiles are essentially driven by the Doppler effect and the concentration is directly related to the absorption depth and to the line strength parameter. The TDLAS may use two distributed-feedback diode lasers emitting, respectively, at 1.88 μm (H_2O and CO_2) and 2.04 μm (CO_2 isotopologues) to record in situ atmospheric spectra of H_2O and CO_2. In the selected spectral regions, molecules are detected simultaneously with a single laser scan. Table 2 presents the chosen lines for the instrument with their respective linestrengths [7, 19].

Our laboratory results are in quite good agreement with the HITRAN database even if the 2004 value for H_2O is worse than the 2000 value: the difference around 6% influences the retrieval by the same factor. The $^{12}C^{16}O_2$ value has been amended between the two versions of the database. The 2004 value is in very good agreement with our experimental data. On the opposite, the CO_2 isotopologues parameters have not been corrected between HITRAN 2000 and 2004. Surprisingly the values for the two carbon dioxide isotopologues are in very good agreement with the experimental ones (around 1% difference). Numerous $^{12}C^{16}O_2$ bands in the 1.6

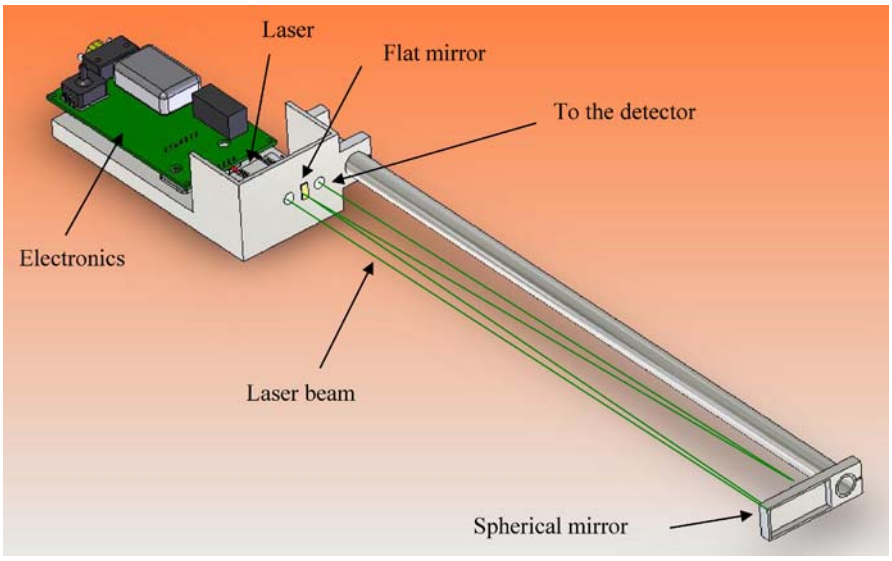

FIGURE 5 Schematic illustration of the TDLAS

Molecule	Band	Transition (J_{KaKc}) upper← (J_{KaKc}) lower	σ_0 (cm^{-1})	Absorption depth (%)	Line strengths (10^{-22} cm^{-1}/(molecule cm^{-2})) Our work	HITRAN 2000	HITRAN 2004
H_2O	$\nu_2+\nu_3$	$1_{11} \leftarrow 1_{10}$	5327.39035	1.2	171	177	182
$^{12}C^{16}O_2$	$(01^12)_I \leftarrow (000)$	R16	5327.24239	0.4	101.3	105.6	102.5
$^{13}C^{16}O_2$	$(20^01)_{II} \leftarrow (000)$	R16	4899.61327	4	0.1038	0.1042	0.1042
$^{18}O^{12}C^{16}O$	$(20^01)_{II} \leftarrow (000)$	P7	4899.56529	0.7	0.0151	0.0147	0.0147

TABLE 2 List of the lines used by the TDLAS instrument. Absorption depths are given for an absorption path length of 1.2 m under Martian pressure and temperature conditions (210 K). Terrestrial isotopic ratios are used for isotopic species

and 2.0 μm regions have demonstrated quite large differences between experimental Fourier Transform measurements and HITRAN data [18]. For example the $(20^01)_{III} \leftarrow(000)$ band of $^{12}C^{16}O_2$ centered around 4850 cm^{-1} shows a mean difference of about 10% for the line strength. On the contrary the $(20^01)_{II} \leftarrow(000)$ band of $^{12}C^{16}O_2$ centered around 4980 cm^{-1} shows a mean difference of about 1% for the line strength. Hence the calculation of this band for $^{12}C^{16}O_2$ seems correct and the values for the $^{13}C^{16}O_2$ and $^{18}O^{12}C^{16}O$ isotopologues are in good agreement with our experimental values.

The next step for this instrument will be the implementation of new diode lasers emitting in the 2.6 μm region in order to measure water vapor isotopologues. This future work is a challenge because absorption depths may be only around 0.02% with an absorption path length of 10 m. Figure 6 presents an example of recorded spectra at 2.67 μm with this kind of new generation laser purchased from Nanoplus. These spectra show the possibility of detecting CO_2 on Earth. The SFP signal is used for frequency calibration. The absorption spectrum is the sum of 10 individual spectra recorded in 5 ms. These results permit obtaining a gas concentration every 0.1 s demonstrating the capabilities of this type of laser for in situ measurements.

5 On the use of a new generation of lasers: the quantum cascade lasers

In the stratosphere, the region of the Earth's atmosphere where the ozone layer is found, a constant increase in the amount of water vapor is observed. Even if the stratosphere appears to be strongly dehydrated, a change in the weak content of H_2O could have a strong effect on the radiative and chemical equilibrium of the stratosphere and further alter ozone recovery. The coupling processes that transport and mix humid tropospheric air masses into the stratosphere, essentially in tropical regions where strong convective events occur, are largely unknown. The in situ measurement of H_2O isotopologues (HDO, $H_2{}^{18}O$ and $H_2{}^{17}O$) can be helpful in addressing this issue, as water–vapor fractionation can be used for diagnosing the transport of an air mass through the upper troposphere and the lower stratosphere, and associated dehydration mechanisms.

The tunable laser probing technique could be a powerful technique for making in situ H_2O isotopologue measurements in the middle atmosphere. The use of tunable diode lasers has demonstrated the possibility of realizing instruments for atmospheric measurements of the main isotopologues. Unfortunately these lasers are limited to the near-infrared region where weak fundamental rovibrational transitions take place. Pb-salt lasers emitting in the mid-IR region need cryogenic cooling. Currently, the most promising tunable mid-infrared sources are quantum-cascade (QC) lasers [8]. We have tested a QC laser from Alpes Lasers emitting in the 6.7 μm spectral region which is available for simultaneous monitoring of all water vapor isotopologues. Spectroscopic measurements of line strengths have been performed [20]. Figure 7 demonstrates the possibility of simultaneously detecting in one scan

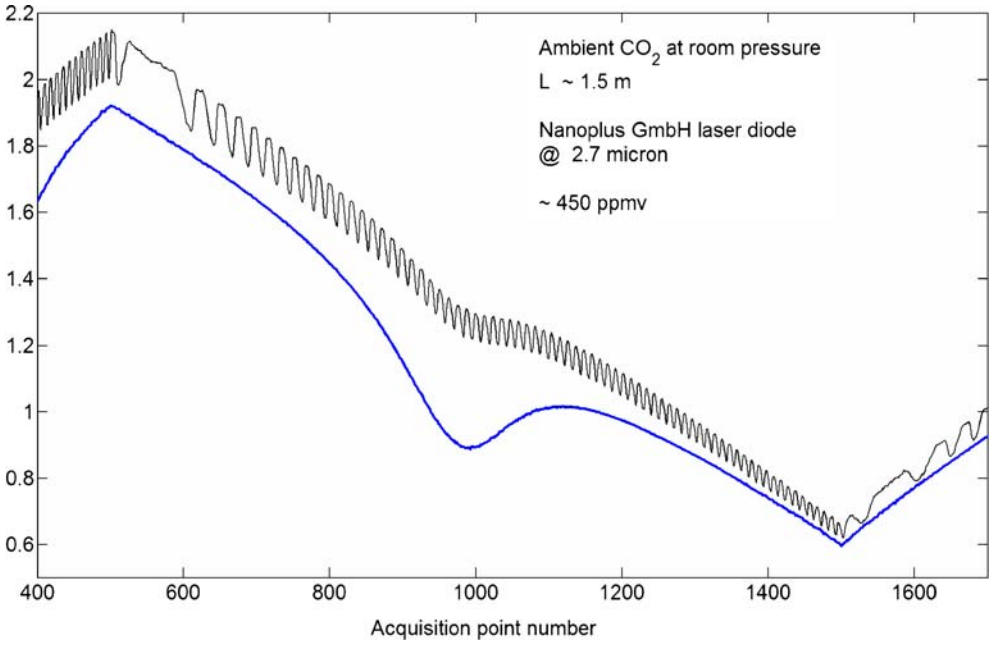

FIGURE 6 Example of recorded spectra with a 2.67 μm Nanoplus laser

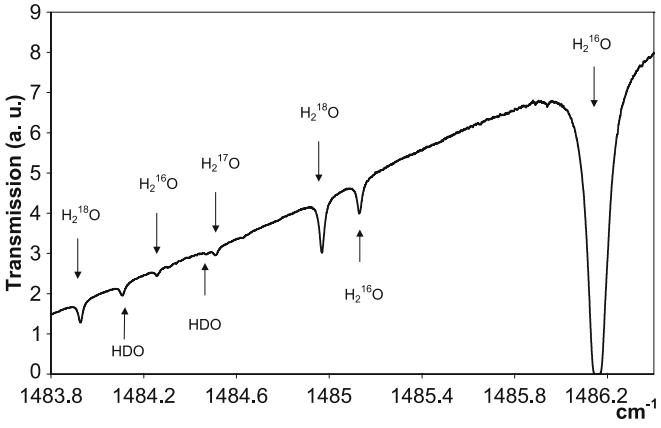

FIGURE 7 Example of a recorded transmission spectrum of air around 1485 cm^{-1} obtained with the quantum cascade laser spectrometer. Pressure is 138 mbar, temperature is 291 K and absorption path length is 48 m

all water vapor isotopologues in air with the same laser. The absorptions can be clearly seen. The water vapor isotopologues concentrations obtained in air were compared [21] with the concentrations obtained with a hygrometer from Honeywell, demonstrating the good reliability of the quantum cascade spectrometer. We now plan to implement, onboard the SDLA, the QC laser to prepare European campaigns devoted to tropical chemistry and dynamics planned for the years 2007 and 2008.

6 Conclusion

We have reported in this paper on the laboratory spectroscopic calibration work required for in-situ TDL sensors to achieve accurate trace gases measurements. A laboratory technique for the precise determination of the spectroscopic parameters of single ro-vibrational lines was described. The lines are those used in the concentration retrieval by high resolution laser based instruments. We have shown that a better knowledge of the spectroscopic parameters directly influences the retrieved concentration, for example for the SDLA balloon-borne instrument which is devoted to the in situ sensing of the middle atmosphere. We have presented the possibility of developing a new generation of instruments based on multi-quantum well laser diodes emitting at room temperature in the 2–3 μm region which cannot be reached with the standard telecommunication laser technology used with the SDLA and μSDLA instruments. The next step will be to use mid-IR quantum cascade lasers to develop more accurate instruments with a smaller path length thanks to their emission in strong fundamental rovibrational transitions. These lasers are the most promising sources. At the moment the need for nitrogen cooling is certainly a drawback for in-situ sensors. However, the development of room-temperature continuous wave quantum cascade lasers is very promising and these lasers are becoming available now.

ACKNOWLEDGEMENTS The work described in this paper was supported by the Centre National d'Etudes Spatiales (CNES), the Programme National de Chimie Atmosphérique (PNCA) of the Institut National des Sciences de l'Univers (INSU) of the Centre National de la Recherche Scientifique (CNRS) and the Région Champagne Ardenne.

REFERENCES

1 G. Durry, G. Mégie, Appl. Opt. **38**, 7342 (1999)
2 E.C. Richard, K.K. Kelly, R.H. Winkler, R. Wilson, T.L. Thompson, R.J. Mclaughlin, A.L. Schmeltekopf, A.F. Tuck, Appl. Phys. B **75**, 183 (2002)
3 D.C. Scott, R.L. Herman, C.R. Webster, R.D. May, G.J. Flesch, E.J. Moyer, Appl. Opt. **38**, 4609 (1999)
4 G. Moreau, C. Robert, V. Catoire, M. Chartier, C. Camy-Peyret, N. Huret, M. Pirre, L. Pomathiod, G. Chalumeau, Appl. Opt. **44**, 5972 (2005)
5 F. D'Amato, P. Mazzinghi, F. Castagnoli, Appl. Phys. B **75**, 195 (2002)
6 G. Durry, A. Hauchecorne, J. Ovarlez, H. Ovarlez, I. Pouchet, V. Zeninari, B. Parvitte, J. Atmosph. Chem. **43**, 175 (2002)
7 T. Le Barbu, B. Parvitte, V. Zéninari, I. Vinogradov, O. Korablev, G. Durry, Appl. Phys. B **82**, 133 (2006)

8 J. Faist, F. Capasso, D.L. Sivco, C. Sirtori, A.L. Hutchinson, A.Y. Cho, Science **284**, 553 (1994)
9 L.S. Rothman, *The HITRAN molecular spectroscopic database and HAWKS*, (2004) Edition. ftp://cfa-ftp.harvard.edu/pub/HITRAN
10 J. Humlicek, J. Quantum. Spectrosc. Radiat. Transf. **27**, 437 (1982)
11 R.R. Gamache, S. Kennedy, R. Hawkins, L.S. Rothman, J. Mol. Struct. **517**, 407 (2000)
12 S.G. Rautian, I.C. Sobel'man, Sov. Phys. Uspekhi **9**, 701 (1967)
13 L. Galatry, Phys. Rev. **122**, 1218 (1961)
14 G. Durry, N. Amarouche, V. Zéninari, B. Parvitte, T. Le Barbu, J. Ovarlez, Spectrochim. Acta A **60**, 3371 (2004)
15 B. Parvitte, V. Zéninari, I. Pouchet, G. Durry, J. Quantum. Spectrosc. Radiat. Transf. **75**, 493 (2002)
16 G. Durry, V. Zéninari, B. Parvitte, T. Le Barbu, F. Lefèvre, J. Ovarlez, R.R. Gamache, J. Quantum. Spectrosc. Radiat. Transf. **94**, 387 (2005)
17 I. Pouchet, V. Zéninari, B. Parvitte, G. Durry, J. Quantum. Spectrosc. Radiat. Transf. **83**, 619 (2004)
18 L. Régalia-Jarlot, V. Zéninari, B. Parvitte, A. Grossel, X. Thomas, P. Von Der Heyden, G. Durry, J. Quantum. Spectrosc. Radiat. Transf. **101**, 325 (2006)
19 T. Le Barbu, V. Zéninari, B. Parvitte, D. Courtois, G. Durry, J. Quantum. Spectrosc. Radiat. Transf. **98**, 264 (2006)
20 L. Joly, B. Parvitte, V. Zéninari, D. Courtois, G. Durry, J. Quantum. Spectrosc. Radiat. Transf. (2006), unpublished
21 L. Joly, V. Zéninari, B. Parvitte, D. Courtois, G. Durry, Opt. Lett. **31**, 143 (2006)